THE JOURNAL OF PHYSICAL CHEMISTRY B

Article

pubs.acs.org/JPCB

The van der Waals Interactions in Sphere-Shell and Cone-Shell Configurations

Americo Boza Troncoso and Edgar Acosta*

Chemical Engineering and Applied Chemistry, University of Toronto, 200 College Street, Room 131, Toronto, Ontario M5S3E5, Canada

ABSTRACT: This work introduces two expressions for the integration of the van der Waals interactions in geometries that are relevant to determining oil solubilization in micelles and the interaction among surfactants in micelles. The first integral applies to the interaction between a sphere and a spherical shell that surrounds the sphere. The second integral calculates the interaction between a truncated cone and the rest of a spherical shell that contains the cone. The new sphere-shell integration method was validated via a comparison between fully predicted and experimental surface tensions of alkanes at room temperature and reproduced the near zero surface tension values that are obtained close to the critical point. The cone-shell integration method was validated, in association with the sphere-shell expression, using a comparison between predicted and experimental cohesive energies for alkanes.

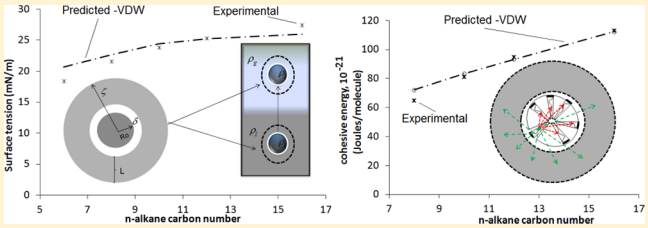

1. INTRODUCTION

van der Waals (VDW) interactions are of universal occurrence due to the fact that they exist between any combinations of molecules.[1,2] Efforts to find expressions that integrate the VDW interactions between different bodies are worthwhile because these VDW interactions are important in many applications including biology, medical science, surface phenomena, and others.[1−10]

The van der Waals interaction between a sphere and a spherical shell can be used to calculate the molecular interactions in oil-swollen micelles and in determining the surface tension of nonpolar fluids. The interaction between a cone and a shell can be used to calculate the interaction among surfactants in micelles, microemulsions, and vesicles. While the literature provides expressions to estimate the VDW interactions between various bodies, there are no explicit expressions to estimate the sphere-shell and cone-shell interactions proposed here.

One of the approaches typically used to calculate VDW interactions is the so-called microscopic approach as originally presented by Hamaker.[11] The microscopic approach estimates the VDW interparticle interaction as a function of their separation distance by summing all of the intermolecular interactions of the interacting bodies following the Hamaker integration approach. Another alternative arises from the use of the so-called Lifshitz macroscopic approach, which results from correlating the electrodynamic and electromagnetic-field fluctuations of the interacting materials.[1,3] From both approaches, the microscopic approach is generally of greater simplicity as compared to the macroscopic one. In addition, the microscopic approach can incorporate the Lifshitz concepts by computing the Hamaker constants in terms of dielectric constants and refractive indices.[2,5] The microscopic approach is employed in this work, using the classical Hamaker constant and the Lifshitz-based Hamaker constant.

Many authors have proposed different expressions to compute the VDW interbody interactions based on the classical Hamaker approach.[1,3,6−8] The interaction between flat surfaces, spheres, sphere-flat surface, parallel cylinders, cylinder-flat surface, and crossed cylinders has been considered by Israelachvili.[1] Among many other relations, Parsegian presented expressions for the interactions of a thin cylinder in a concentric cylinder, coaxial thin roads, and of a circular disk with a rod.[3] Gu and Li presented a method to calculate the VDW interaction between a spherical particle and a cylinder to overcome deficiencies caused by simplifying assumptions previously made to emulate this interaction with other interbody configurations.[9] Kirsh also derived expressions to calculate the retarded and unretarded VDW interaction of a sphere with an infinite cylinder.[10] Su and Flumerfelt presented an integration method related to the sphere-shell interactions considered in this work.[12] However, these researches calculated the energy associated with extracting a liquid sphere from a continuous liquid phase as a method to estimate the surface tensions of *n*-alkanes.

The integration of the VDW interactions is very important in understanding solubilization in micelles and microemulsion systems. In an earlier effort to explain the thermodynamics of microemulsion, Winsor introduced a balance of interaction energies between the surfactant, oil, and water in the so-called *R* ratio.[13] However, the estimation of these energies has never been performed due to the lack of quantitative expressions for these interactions. The integration methods introduced here have the potential to fill this gap in the calculation of molecular interactions in surfactant−oil−water systems.

Received: June 5, 2012
Revised: October 20, 2012
Published: October 24, 2012

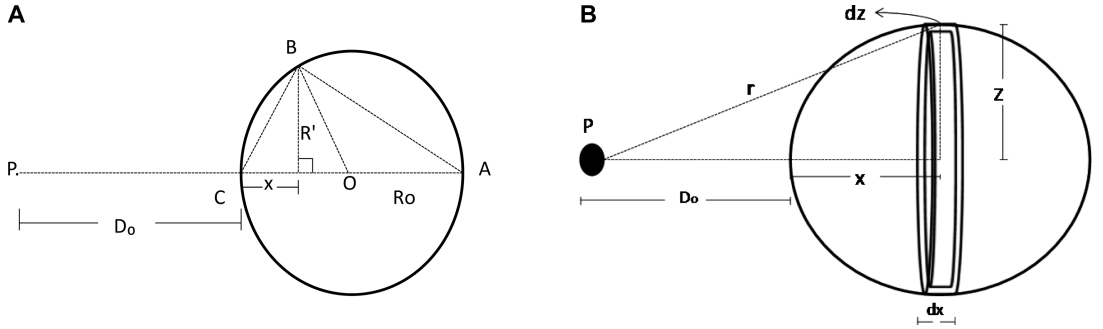

Figure 1. (A) Schematic illustration of the chord theorem. A right-angled triangle ABC is inscribed in a semicircle. The drawing is used to establish a relation between R' and R_o to use in the VDW integration. (B) Interaction of a hard sphere molecule, located at a point P, with a circular ring of cross-section area dx dz. Z is the radius of the ring, and D_o is the distance between the molecule and the sphere.

The expression developed in this work for the integration of the VDW interactions in a sphere-shell configuration was used to predict the surface tension of *n*-alkanes at different temperatures. These surface tensions were compared to experimental values to assess the validity of the integration method. The expression developed for the integration of the VDW interactions in a cone-shell configuration was used in combination with the sphere-shell equation to obtain the cohesive energies of *n*-alkanes. These predicted values were compared with experimental data. It should be emphasized that the main objective of this work was not to provide a new approach to estimate surface tension or cohesive energies but to introduce and validate methods to integrate interaction potentials in sphere-shell and cone-shell configurations that are relevant to various applications, including oil solubilization in micelles, vesicle and liposome formation, and others. Both equations have essentially no adjustable parameters other than the separation between cones in the cone-shell interaction. Even the adjusted separation distance was found to be roughly 96% of the literature value[1,12]

2. MODEL DEVELOPMENT

The interaction potential between two molecules can be written as:[5]

$$w(r) = \frac{-C}{r^n} \tag{2.1}$$

for $r > \sigma$, while for $r < \sigma$, $w(r)$ becomes infinite, where σ is the so-called hard sphere diameter, C is the interaction coefficient, and r represents the distance between molecules. The VDW interaction is a collective term used to refer to Keesom, Debye, and London dispersion interactions. All of them decrease with the inverse sixth power of the distance in eq 2.1. For particle−particle or particle−surface interactions, the Keesom and Debye contributions to the VDW forces can be disregarded unless the particle has a permanent dipole.[5] With this consideration, the constant C can be expressed in terms of the London dispersion interactions, as follows:[5]

$$C = \frac{3\alpha_{PA}\alpha_{PB}I_AI_B}{(4\pi\varepsilon_o)^2(I_A + I_B)} \tag{2.2}$$

where α_{PA} and α_{PB} are the molecular polarizabilities of the interacting bodies A and B. I_A and I_B are the first ionization potentials of the interacting molecules. ε_o is the vacuum permittivity. To relate the interaction of molecular pair potentials to the interactions of particles, we could follow the microscopic Hamaker approach.[1] This method consists of integrating the pair interaction potential between molecules of two bodies to obtain the interaction between two macroscopic bodies, such that:[10,11]

$$V(r) = \int_{V_2}\int_{V_1} \frac{-C\rho_1\rho_2\, dV_1\, dV_2}{r^6} \tag{2.3}$$

ρ_1 and ρ_2 are the molecular densities and V_1 and V_2 are the volumes of the interacting bodies. This equation is also known as the Hamaker equation, which gives raise to the Hamaker constant:[1]

$$A = \pi^2 C\rho_1\rho_2 \tag{2.4}$$

Equations 2.2 and 2.4 can be combined to obtain the classical Hamaker constant. The Hamaker constant can also be calculated using a continuum approach based on the Lifshitz theory.[1] The nonretarded Hamaker constant for pure components interacting across a medium[3] can be calculated using the following equation:[1]

$$A_{ls}(T) = \frac{3}{4}\kappa T\left(\frac{\varepsilon_1 - \varepsilon_3}{\varepsilon_1 + \varepsilon_3}\right)^2 + \frac{3h\gamma_e}{16\sqrt{2}}\frac{(n_1^2 - n_3^2)^2}{(n_1^2 + n_3^2)^{3/2}} \tag{2.5}$$

T is the absolute temperature, k is the Boltzmann constant, ε is the dielectric constant, h is the Planck's constant, γ_e is the characteristic absorption frequency, and n is the refractive index. The temperature dependence of the dielectric constant for liquids can be estimated using the following correlation:[14]

$$\varepsilon_l(T) = a + bT + cT^2 + dT^3 \tag{2.6}$$

where a, b, c, and d are empirical constants. The temperature-dependent dielectric constant of alkanes can also be calculated using the Clausius−Mosotti equation:[15]

$$\frac{\varepsilon - 1}{\varepsilon + 2} = \rho_m\frac{4\pi N\alpha_p}{3} \tag{2.7}$$

where ρ_m is the molar density, N is Avogadro's number, and α_p is the polarizability of the molecule. The refractive index can be estimated using the following equation.[12]

$$\eta = \sqrt{\varepsilon} \tag{2.8}$$

2.1. Sphere-Shell Interactions. The procedure to calculate the VDW attraction between a sphere and a spherical shell consists of establishing a relationship to calculate the interaction between a hard sphere molecule located at a point P and a sphere, as sketched in Figure 1A. This is accomplished by summing the VDW interaction energy between the molecule located at P and all of the molecules in the sphere. Figure 1B

dx.doi.org/10.1021/jp305534d | J. Phys. Chem. B 2012, 116, 14051−14061

presents the differential element of volume of the sphere used to integrate the VDW interactions.

From Figure 1A, the following relation is established:

$$R'^2 + (R_o - x)^2 = R_o^2 \tag{2.9}$$

After simplifying the expression:

$$R' = \sqrt{2R_o x - x^2} \tag{2.10}$$

Referring to Figure 1B and by placing the adequate limits of integration to the volume element $2\pi z\ dz\ dx$, the interaction potential between a molecule and a sphere has the following form:

$$\varphi(R_o) = \int_0^{2R_o} \int_0^{\sqrt{2R_o x - x^2}} \frac{-\rho_1 C 2\pi z\ dz\ dx}{r^n} \tag{2.11}$$

The distance r between the molecule at P and the volume element of the sphere is deduced from Figure 1B so that the interaction potential is

$$\varphi(R_o) = \int_0^{2R_o} \int_0^{\sqrt{2R_o x - x^2}} \frac{-\rho_1 C 2\pi z\ dz\ dx}{[(D_o + x)^2 + z^2]^{n/2}} \tag{2.12}$$

The integration of eq 2.12 provides the following algebraic equation:

$$\varphi(R_o) = \frac{-\rho_1 C 2\pi}{(2-n)}\left[\frac{(D_o + 2R_o)^{4-n} - D_o^{4-n}}{(D_o + R_o)(4-n)} - \frac{(D_o + 2R_o)^{3-n} - D_o^{3-n}}{(3-n)}\right] \tag{2.13}$$

Equation 2.13 can be used to calculate the interaction potential of a sphere with a molecule for any given D_o and n. To proceed to a complete solution of the two-body interaction, eq 2.13 can be further simplified taking $n = 6$ for unretarded VDW interactions.

$$\varphi(R_o) = \frac{-\rho_1 C 4\pi R_o^3}{3D_o^3(D_o + 2R_o)^3} \tag{2.14}$$

Rearranging:

$$\varphi(R_o) = \frac{-\rho_1 C 4\pi R_o^3}{3[(D_o + R_o)^2 - R_o^2]^3} \tag{2.15}$$

Using a different approach, Kirsh found the same expression for the VDW molecule−sphere interaction.[16] The term $(D + R_o)$ in eq 2.15 represents the distance from the center of the sphere to any point outside of it, which can be replaced by any arbitrary term such as ζ. To establish a distance between the sphere and a volume element of a shell enclosing the sphere, one could extend r from the center of the sphere to the outer diameter of the shell, as depicted in Figure 2.

The interaction of a sphere with the spherical shell can be obtained using eq 2.15 by integrating the interactions of an element of volume of the spherical shell containing $\rho_2 4\pi\zeta^2\ d\zeta$ molecules, following the Hamaker approach:

$$W_H(R_o) = \frac{-\rho_1\rho_2 16\pi^2 R_o^3 C}{3} \int_{R_o+\delta_T}^{R_o+\delta_T+L} \frac{\zeta^2\ d\zeta}{(\zeta^2 - R_o^2)^3} \tag{2.16}$$

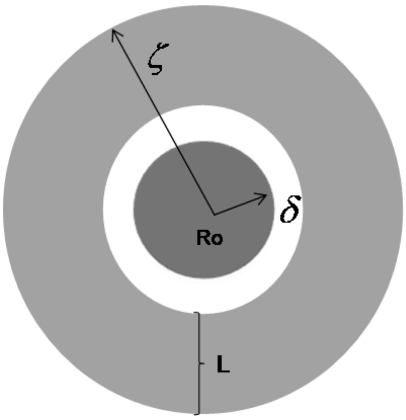

Figure 2. Cross-section of a sphere enclosed by a spherical shell. R_o is the radius of the sphere, and δ is the interfacial cut off distance between the sphere and the shell. L is the length of the shell that surrounds the sphere. ζ represents the distance from the center to the external diameter of the shell.

In eq 2.16, the limits of integration are established considering the sphere size R_o, the length (L) of a shell that surrounds the sphere. δ_T is the interfacial separation cut-off distance, as defined in the literature.[1] This integration can be solved numerically with various math solvers.

2.2. Cone-Shell Interactions. The interaction potential of a cone with a shell can be used to calculate the lipophilic interactions between a surfactant and the rest of surfactants tails contained in a micelle, as illustrated in Figure 3A. One of the possibilities to represent this interaction is to assume that it occurs between a truncated cone and the remaining part of a micelle that contains the conical section, as depicted in Figure 3B.

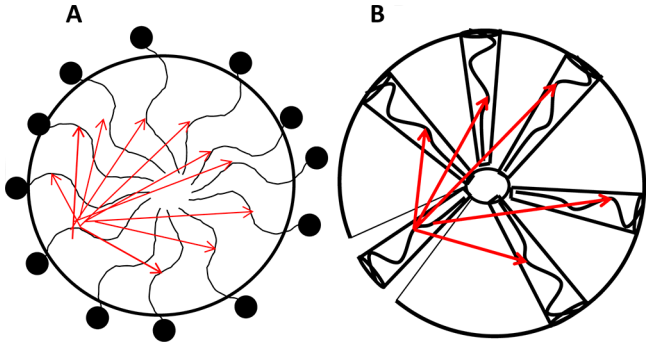

Figure 3. (A) Graphical representation of the lipophilic interactions between a surfactant tail and the rest of the tails contained in a micelle. (B) Truncated cone-shell configuration assumed to estimate the lipophilic interactions of a hypothetical molecule representing a surfactant tail with the rest of molecules contained in a micelle.

One of the difficulties in undertaking the cone-shell integration is to ensure that the molecules are properly packed. In reality, some molecules would be able to stretch closer to the center of the sphere, while others remain away from the center of the sphere. The best way to represent this packing restriction and maintain a homogeneous packing density is to restrict all of the molecules from the center of the sphere. Experimentally, it has been determined that in micelles, the surfactants only stretch 80% of its length.[17−19] In this work, it is assumed that the radius of the excluded volume at the center of the sphere is 20% of the length of the molecule.

dx.doi.org/10.1021/jp305534d | J. Phys. Chem. B 2012, 116, 14051−14061

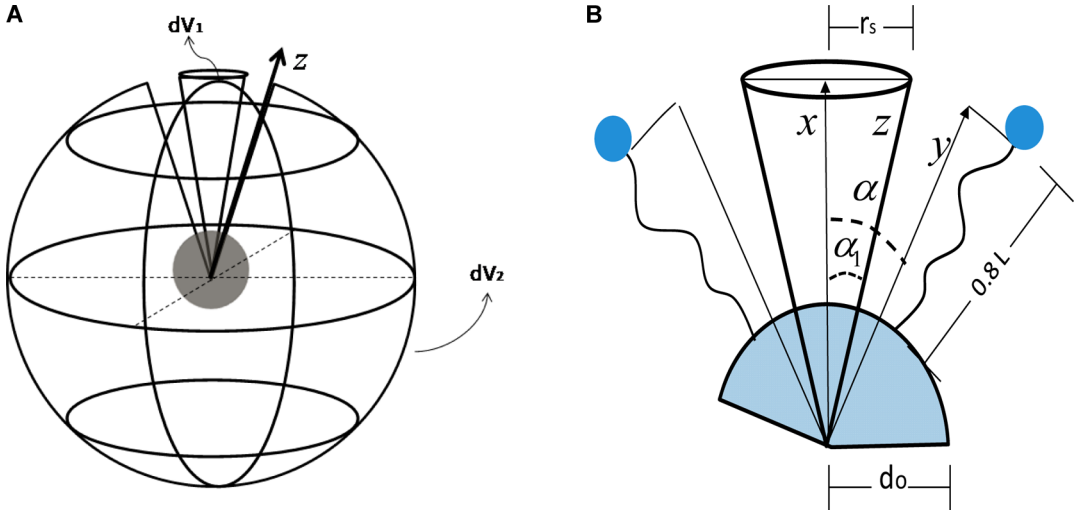

Figure 4. (A) Geometrical arrangement used to calculate the cone-shell VDW interaction potential. dV_1 and dV_2 are defined to calculate the truncated cone and the coneless shell volumes, respectively. (B) Cross-sectional view illustration of the cone-shell interaction. α_1 defines the angle between the axes x and z. α defines the angle between the axes x and y. d_o is the radius of the empty hole at the center of the cone. $0.8L$ represents the shell length, and r_s represents the cone radius.

The approach used to estimate the VDW interaction of a truncated cone with a shell consists of defining two elements of volume in spherical coordinates, one for the cone and the other for the rest of the spherical shell, as shown in Figure 4A.

The volume element of the conical section dV_1 can be calculated using the following equation.

$$dV_1 = 2\pi z^2 \sin(\phi)\, d\phi\, dz \tag{2.17}$$

z can be redefined in terms of x according to Figure 4B as follows:

$$x = z\cos(\alpha_1) \tag{2.18}$$

dV_1 can be integrated with respect to the angle ϕ to its boundary condition α_1. In addition, it can be written in terms of x using eq 2.18 so that eq 2.17 is expressed as:

$$dV_1 = \frac{2\pi x^2[1 - \cos(\alpha_1)]\, dx}{[\cos(\alpha_1)]^3} \tag{2.19}$$

The angle α_1 can be defined by geometrical means referring to Figure 4B:

$$\alpha_1 = a\tan\left(\frac{r_s}{0.8L + d_o}\right) \tag{2.20}$$

d_o is the radius of the empty spherical hole defined previously as being 20% of the length L of a hypothetical straight alkane chain, which could represent a surfactant tail. r_s represents the external radius of the truncated cone and is calculated considering the surface area occupied by the cone as:

$$r_s = \sqrt{\frac{A_o}{\pi}} \tag{2.21}$$

The surface area of the cone A_o is calculated considering maximum molecular packing in the shell so that the expression is given by:

$$A_o = \frac{4\pi(0.8L + d_o)^2}{N_s} \tag{2.22}$$

The shell's aggregation number N_s is calculated using the volume of the shell divided by the volume occupied by a molecule, as follows:

$$N_s = \frac{4\pi[(0.8L + d_o)^3 - d_o{}^3]}{3V_o} \tag{2.23}$$

where V_o is the volume of a single molecule (m^3/molecule), which can be calculated from the density of the desired component.

The volume element dV_2, of the coneless shell of Figure 4A, is defined using an expression similar to eq to 2.17 but using different variables in accordance to Figure 4B:

$$dV_2 = 2\pi y^2 \sin(\alpha)\, dy\, d\alpha \tag{2.24}$$

The Hamaker integration, eq 2.3, over the truncated cone and the coneless shell provides the interaction potential of these two bodies, giving the following expression:

$$\Gamma_H = -\int_{d_o}^{d_o+0.8L}\int_{d_o}^{d_o+0.8L}\int_{\alpha_2}^{\pi}\left\{4\pi^2\rho^2 C y^2 x^2 \sin\alpha\left[\frac{1}{[\cos(\alpha_1)]^3} - \frac{1}{[\cos(\alpha_1)]^2}\right] d\alpha\, dy\, dx\right\}\Big/\left\{[x^2 + y^2 - 2xy\cos(\alpha)]^3\right\} \tag{2.25}$$

The limits of integration of the x- and y-axis, cone and shell, develop from the radius of the excluded volume d_o to $0.8L$. The distance between the differential volume element dV_1 in the cone and the differential volume element dV_2 in the coneless shell is given by the cosine law, in accordance to Figure 4B. α_2 represents the limit of integration of the shell and is calculated using the following relation.

$$\alpha_2 = \alpha_1 + f\alpha_1 \tag{2.26}$$

The term f in eq 2.26 is introduced to account for the interfacial separation angle between the cone and the shell. Unfortunately, for this geometry, it is not possible to define a proper separation distance δ. The treatment of this equation is further explained in section 3.2.

dx.doi.org/10.1021/jp305534d | J. Phys. Chem. B 2012, 116, 14051−14061

Table 1. Selected Pure Component Properties for the Calculation of the Classical and Modified Lifshitz Hamaker Constants

component	g/cm^3 at 20 °C ρ_g[a]	g/cm^3 at 20 °C ρ_l[a]	I[b] (eV)	α[c] (Å^3)	γ_e[d] (10^{15} s^{-1})	A[e] (10^{-20} J) at 20 °C
C6	5.80×10^{-4}	0.7022	10.12	11.83	2.98	4.055
C8	6.54×10^{-5}	0.73033	10.03	15.52	2.97	4.484
C10	7.46×10^{-6}	0.74936	9.95	19.22	2.98	4.812
C12	8.17×10^{-7}	0.7733	9.93	22.91	2.99	5.02
C16	1.03×10^{-8}[f]	0.7733[g]	9.91	29.76[h]	2.94	5.192

[a]NIST webbook.[20] [b]Melton and Joy.[21] [c]Miller and Savchik.[22] [d]Su and Flumerfelt.[12] [e]Calculated using eq 2.5. [f]Calculated using the PR-SV EOS. [g]Outcalt et al.[23] [h]Approximated using a group contribution approach.[1]

3. RESULTS

In this section, the interaction potential of a sphere with a shell is associated with the surface tension of normal *n*-alkanes ranging from hexane to hexadecane (C6, C16). In the second part of this work, the interaction potential of a cone with a shell is combined with the interaction potential of a sphere with a shell to predict the cohesive energy of *n*-alkanes. The interaction potentials are computed using either the classical Hamaker constant or the Lifshitz-based Hamaker constant.

To arrive at the results presented in the subsequent sections, different component properties as well as parameters were calculated or obtained from the literature. Table 1 presents a summary of the input data used for the calculations of the interactions at 20 °C. The temperature dependence of the dielectric constant is calculated using eq 2.6 and the parameters summarized in Table 2.

Table 2. Parameters To Calculate the Temperature Dependence of the Dielectric Constant of *n*-Alkanes[a]

	A	B	C	D	range T (K)
C6	1.9768	7.09×10^{-4}	-3.45×10^{-6}	0	293.2−473.2
C8	2.259	-8.42×10^{-4}	-7.58×10^{-7}	0	233.2−393.2
C10	2.4054	-1.54×10^{-3}	4.46×10^{-7}	0	253.2−393.2
C12	2.3697	-1.22×10^{-3}	-3.64×10^{-17}	0	283.2−363.2
C16	2.3861	-1.16×10^{-3}	2.56×10^{-16}	0	293.2−363.2

[a]Data from ref 14.

For all cases, the alkane chain lengths were calculated using the relation proposed by Tanford.[18,19] The interfacial separation distance δ in the liquid phase was considered to be 0.165 nm at 25 °C.[1] However, its temperature dependence is proposed to follow an analogous form of a relation proposed in the literature.[12]

$$\delta_T = \delta\left(\frac{\rho_{25}}{\rho_T}\right)^{1/3} \tag{3.1}$$

δ_T is the interfacial separation distance at a temperature T, ρ_{25} is the density of a component at 25 °C, and ρ_T is the density at the desired temperature T. Additionally, the interfacial separation distance between a liquid drop and its surrounding gas phase was assumed to be the average distance between those in the liquid and gas phases. The numerical solution of the integrals of eqs 2.16 and 2.25 was implemented in Mathcad version 15.0. In most cases, an adaptive quadrature numerical integration method was selected.[24]

3.1. Sphere-Shell. Tables 3 and 4 show the interaction potentials between an oil drop (size R_o) with shell layers of varying thickness at 20 °C. W_H and W_{H-LS} represent calculations made with the sphere-shell interaction potential using the classical Hamaker constant A and using the Lifshitz-based Hamaker constant A_{ls}, respectively. For calculations here, it was established arbitrarily that a layer is equivalent to a hexadecane chain length ($L \approx 2.17$ nm).

As follows from Table 3, fixed *n*-octane drop sizes of 12.5 or 40 nm interacting with shell layers of increasing thickness do not produce any significant increase in the interaction potentials W_H and W_{H-LS}. This pattern is also observed in Table 4 when evaluating the same interbody interactions for hexadecane. This fact let us establish and assume that a shell length of about 2.17 nm is enough for all practical purposes and subsequent simulations.

Figures 5A,B shows the variation of the unretarded VDW interaction potentials of a sphere of increasing drop size with a shell for various *n*-alkanes at 20 °C. The calculation of the potentials in Figure 5A was evaluated using the classical microscopic approach of Hamaker, while the plots generated in Figure 5B were calculated using the microscopic approach of Hamaker but with Hamaker constants modified according to the Liftshitz theory. Comparing Figure 5A,B, the interaction potentials calculated with the Lifshitz-based Hamaker constant produce stronger interactions than those calculated with the classical Hamaker constant.

Other applications of interest for VDW integrals might involve situations where the separation distances are larger than the minimum interfacial separation ($\delta = 0.165$ nm) considered in this work. At larger separations, retardation effects are expected to be significant. To assess these retardation effects, the Appendix shows the development of an integral for VDW interactions in a sphere-shell configuration including the retardation effects estimated via the Overbeek approximation. For an example of a 5 nm hexadecane drop and a $1 \times L$ shell, there was very little difference between the unretarted and the

Table 3. *n*-Octane Interaction Potentials of a Sphere with Varying Shell Thicknesses

shell thickness	R_o (nm)	$-W_H$(Joules)	$-W_{H\text{-}LS}$(Joules)	R_o (nm)	$-W_H$(Joules)	$-W_{H\text{-}LS}$(Joules)
L	12.5	75.20×10^{-18}	90.09×10^{-18}	40	76.30×10^{-17}	91.51×10^{-17}
$2 \times L$	12.5	75.40×10^{-18}	90.44×10^{-18}	40	76.60×10^{-17}	91.80×10^{-17}
$10 \times L$	12.5	75.50×10^{-18}	90.57×10^{-18}	40	76.70×10^{-17}	91.90×10^{-17}
$20 \times L$	12.5	75.50×10^{-18}	90.57×10^{-18}	40	76.70×10^{-17}	91.90×10^{-17}

dx.doi.org/10.1021/jp305534d | J. Phys. Chem. B 2012, 116, 14051−14061

Table 4. *n*-Hexadecane Interaction Potentials of a Sphere with Varying Shell Thicknesses

shell thickness	R_o (nm)	$-W_H$(Joules)	$-W_{H\text{-}LS}$(Joules)	R_o (nm)	$-W_H$(Joules)	$-W_{H\text{-}LS}$(Joules)
L	12.5	86.12×10^{-18}	103.10×10^{-18}	40	87.48×10^{-17}	104.70×10^{-17}
$2 \times L$	12.5	86.40×10^{-18}	103.50×10^{-18}	40	87.81×10^{-17}	105.00×10^{-17}
$10 \times L$	12.5	86.46×10^{-18}	103.51×10^{-18}	40	87.86×10^{-17}	105.10×10^{-17}
$20 \times L$	12.5	86.46×10^{-18}	103.51×10^{-18}	40	87.86×10^{-17}	105.10×10^{-17}

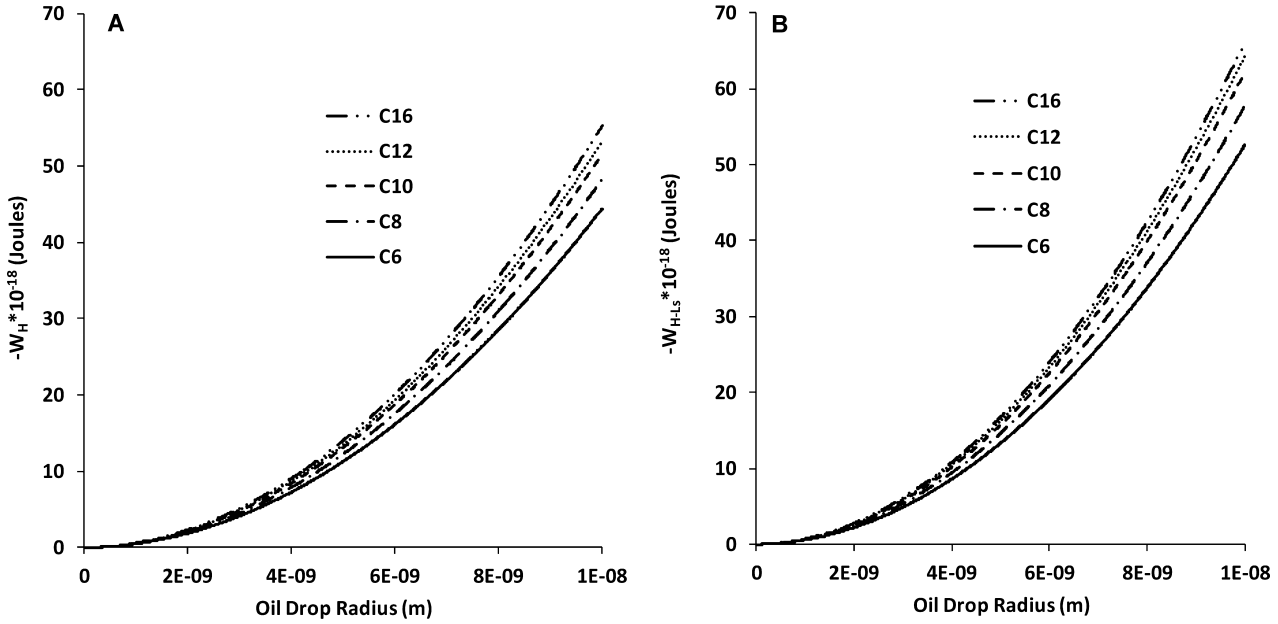

Figure 5. (A) Pure component interaction potential of a sphere with a shell at 20 °C for *n*-alkanes calculated using the classical Hamaker constant. (B) Pure component interaction potential of a sphere with a shell at 20 °C for *n*-alkanes calculated using the Lifshitz-based Hamaker constant.

retarded interaction potential for interfacial separation distances smaller than 10 nm.

The predictions of Figure 5A,B represent the work needed to pull a liquid drop from its solution and into vacuum air, which should represent a good approximation to estimate surface tensions at low temperatures, away from the critical point. However, a proper calculation of equilibrium surface tension requires the work needed to take a liquid drop from its continuum liquid phase into a gas phase saturated with the vapor of the oil, as described schematically in Figure 6.

From the previous analysis, depicted in Figure 6, the surface tension of a liquid can be estimated from the following equation:

$$\gamma = \frac{-W(R_o) + \Omega(R_o)}{4\pi[R_o^2 + (R_o + \delta)^2]} \tag{3.2}$$

where $W(R_o)$ is the sphere-shell interaction potential of a liquid drop with its surrounding liquid and $\Omega(R_o)$ is the interaction potential of the same liquid drop with its surrounding vapor phase at equilibrium. The interaction potentials of the alkane drop in the liquid and gas phases were estimated considering constant VDW dispersion coefficient but considering different densities in both phases. The molecular polarizabilities are known to be weak functions of temperature so they were assumed to be constant for all purposes during the calculations.[14]

To calculate the Lifshitz-based Hamaker constants, the temperature dependence of the dielectric constants in the liquid phase was estimated using eq 2.6, and in the gas phase, eq 2.7 was used. The refractive index is a simple function of the dielectric constant, and the characteristic absorption frequencies were assumed to be constant.[12]

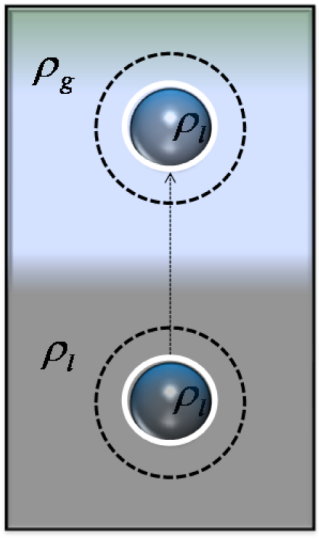

Figure 6. Process of transferring an oil drop from a fixed position in a continuum liquid phase to a fixed position in its vapor phase at equilibrium. The dashed lines represent the surrounding shell of molecules where the interactions are significant for surface tension determination.

Figure 7A shows alkane surface tension predictions at 20 °C with varying cluster sizes estimated using eq 3.2 on the basis of eq 2.16 (classical Hamaker constant). The predictions of Figure 7B were also performed using eq 3.2 on the basis of eq 2.16 but with Lifshitz-based Hamaker constants. Both predictions in Figure 7A,B show that the surface tension approaches a constant

dx.doi.org/10.1021/jp305534d | J. Phys. Chem. B 2012, 116, 14051−14061

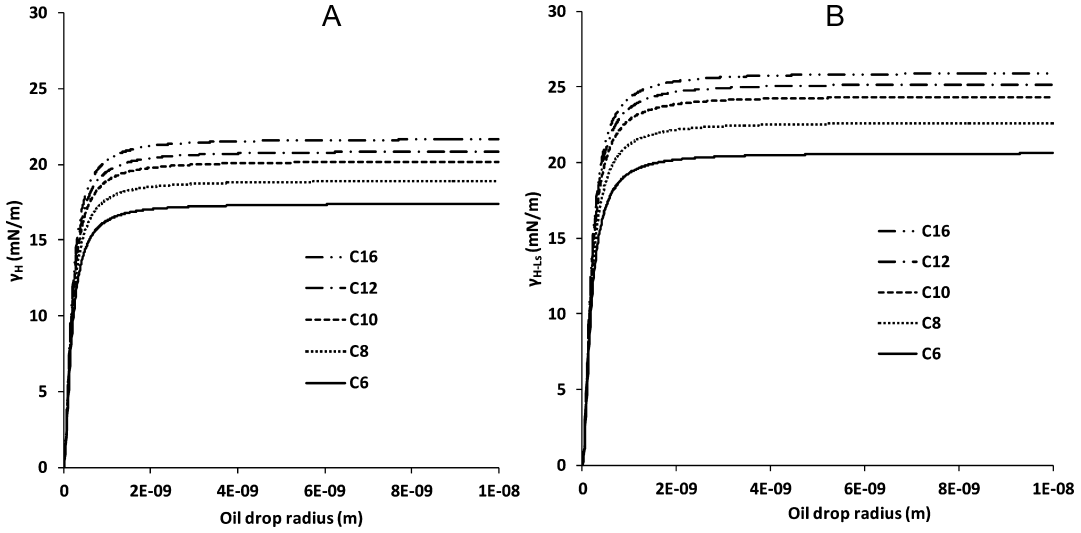

Figure 7. (A) Alkane surface tension predictions at 20 °C using eq 3.1 with Hamaker constants described in eq 2.4. (B) Alkane surface tension predictions at 20 °C using eq 3.1 with Hamaker constants described in eq 2.5.

value as the drop size increases. Similar results have been found by Su and Flumerfelt following a different approach that does not consider the sphere-shell interaction and the liquid–vapor interaction.[12] Figure 7A,B suggests that macroscopic measurements of surface tension apply to drops larger than 1 nm. These predictions are also consistent with the predictions of Israelachvili and Tolman that the surface tension of small clusters differs from the surface tension measured at macroscopic interfaces.[1,25] This discrepancy can be attributed to the way the sphere interacts with its shell. For big enough spheres ($R_o \geq 1$ nm), the sphere-shell interaction approaches that of two parallel shells, and two parallel shells approach the interaction of two parallel plates. The macroscopic measurements of surface tensions are often related, via the Hamaker constant, with the interaction of two parallel plates.[1]

The surface tensions predicted using the sphere-shell interaction potential can be compared to experimental surface tension values reported in the literature.[26,27] Figure 8 shows experimental surface tensions for different alkanes as well as predictions based on the sphere-shell potential using the classical and Lifshitz-based Hamaker constants. All predictions were performed at cluster sizes that were big enough to provide constant surface tension predictions (R_o = 10 nm). At 20 °C, the predictions of eq 3.2 obtained with the modified Lifshitz-based Hamaker constant produce a closer match with the experimental values than the predictions obtained with the classical Hamaker constant. The average error for predictions obtained with the Lifshitz-based Hamaker is less than 3%, as compared to about 12% for calculations using the classical Hamaker constant. These results are slightly better when compared to estimations performed based on the typical two-plate assumption and others proposed in the literature.[12]

Following the procedures previously described, predictions of *n*-octane surface tension were evaluated from 0 °C to its critical point. To perform these predictions, using the classical Hamaker constant, the alkane saturation properties were obtained from the NIST webbook.[20] As seen in Figure 9, the predictions based on the classical Hamaker constant reproduce the experimental behavior at temperatures from about 45 to 100 °C and the near zero surface tension at the critical point. On the other hand, surface tension predictions based on the use of the Lifshitz-based Hamaker constant reproduces the

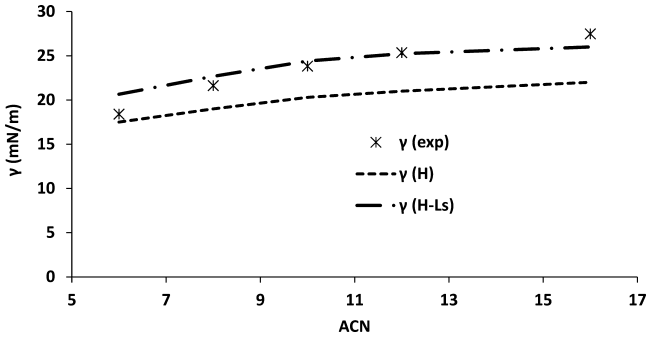

Figure 8. Surface tension of *n*-alkanes at 20 °C as a function of the alkane carbon number (ACN). The dashed line represents the predictions with the classical Hamaker constant $[\gamma(H)]$. The dot dashed line represents the prediction obtained using the Lifshitz-based Hamaker constant $[\gamma(H - L_s)]$. The asterisks represent the experimental data obtained from ref 27.

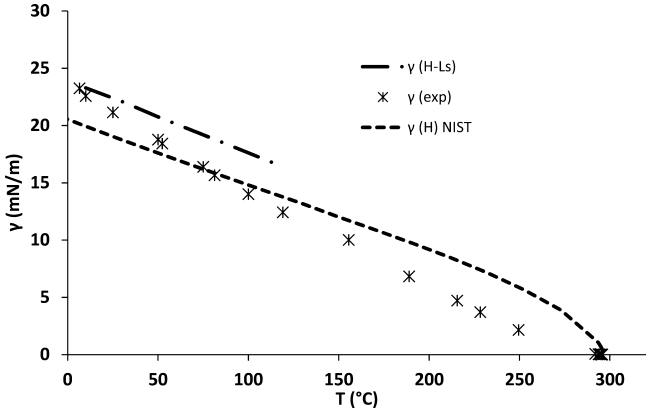

Figure 9. Surface tension of *n*-octane predicted using the classical Hamaker constant $[\gamma(H)]$ and the Lifshitz-based Hamaker constant $[\gamma(H - L_s)]$. Predictions from 0 °C to its critical point. Experimental surface tension data $[\gamma(\exp)]$ obtained from refs 26 and 27.

experimental data below room temperature. It was not possible to evaluate the surface tension at elevated temperatures using the Lifshitz-based Hamaker constant due to lack of parameters for temperatures above 120 °C.

dx.doi.org/10.1021/jp305534d | J. Phys. Chem. B 2012, 116, 14051–14061

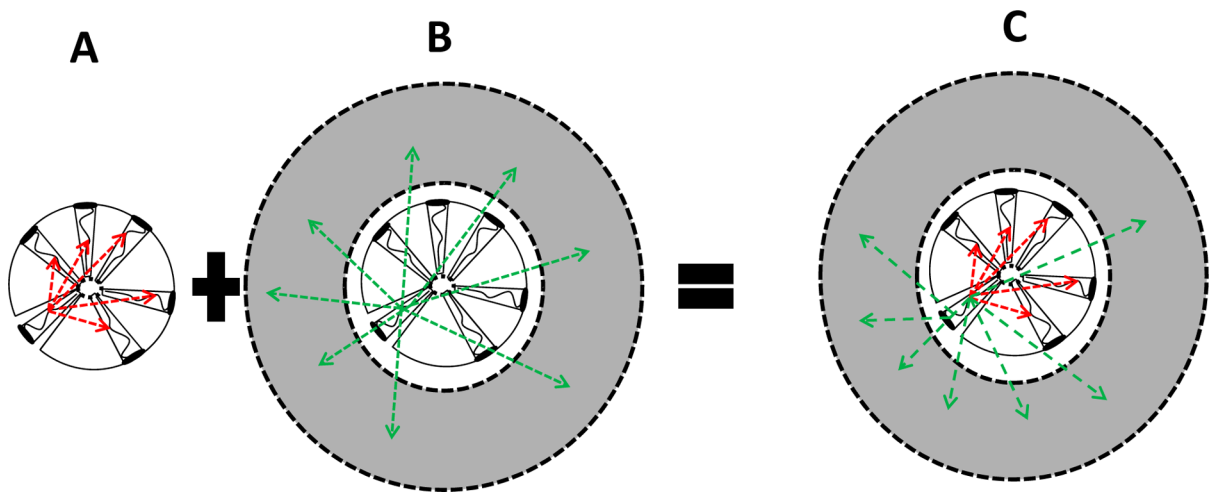

Figure 10. (A) Graphical depiction of the interactions of a cone with a coneless shell represented with red arrows. (B) The cone-containing shell is inserted into the bigger shell. The cone interacts with the shell that surrounds the cone-containing shell as represented in part B. (C) The cone interacts with the coneless shell and the external shell.

3.2. Truncated Cone-Shell. To calculate the cohesive energy of *n*-alkanes, an idealized micellelike structure of alkane molecules enclosed by a shell of the alkane was considered. To evaluate the cone-shell interaction potential, let us consider the graphical representation shown in Figure 10. The first sketch on the left denoted with A represents the interaction of a hypothetical surfactant tail with the rest of the tails conformed in a spherical micelle. These interactions can be calculated using the cone-shell interaction potential.

For an alkane molecule representing a surfactant tail, the interactions indicated with the red arrows in this first diagram represent a fraction of its interactions (Γ). To count all of its interactions, it is also necessary to consider its interactions with the molecules that surround the hypothetical micelle, represented with the green dotted arrows. The molecules that surround the micelle can be assumed to have a shell conformation as indicated in Figure 10B. The interactions of a molecule conformed in a micelle, as described in Figure 10C, with a surrounding shell can be calculated using the sphere-shell interaction potential so that its cohesive energy goes as:

$$U = \Gamma + \frac{W(R_o)}{N_s} \tag{3.3}$$

From the evaluation of *n*-alkane surface tensions around room temperature, it was observed that the sphere-shell interaction potential using the Lifshitz-based Hamaker constant matches the experimental observations reasonably well. On the basis of this finding, eq 3.3 was evaluated in terms of the Lifshitz Hamaker constant around room temperature. Because the sphere-shell interaction potential needed to be used to estimate the interaction between the two shells illustrated in Figure 10C, the cone-containing shell was assumed to be a sphere of radius L. As discussed earlier, large enough spheres (R_o > 1 nm) tend to behave as shells because the large separation distance between the center of the sphere and the outer shell makes that interaction negligible. Furthermore, the volume difference between a solid sphere of radius L and a shell with a $0.2L/1L$ of internal/external shell radius is less than 0.8%. N_s is the alkane aggregation number within the hypothetical micelle calculated assuming maximum packing conditions, as detailed in section 2.2. In section 3.1, it was shown that the extent of the shell that encloses an oil drop or a micelle could be restricted to a layer of about 2.17 nm.

The cohesive energy of liquids around room temperature at low pressures can be related to the enthalpies of vaporization using the following relation.[5,28]

$$-U \approx \Delta U^V = \Delta H^V - RT \tag{3.4}$$

where ΔH^V is the enthalpy of vaporization, ΔU^V is the difference between the internal energies of the vapor and liquid, and R represents the universal gas constant. The cohesive energy of different alkanes was predicted using eq 3.3 and compared to cohesive energies calculated from experimental latent heats of vaporization at 25 °C.[29]

Figure 11 shows that there is close agreement between the predicted cohesive energy and the experimental values. Hexane

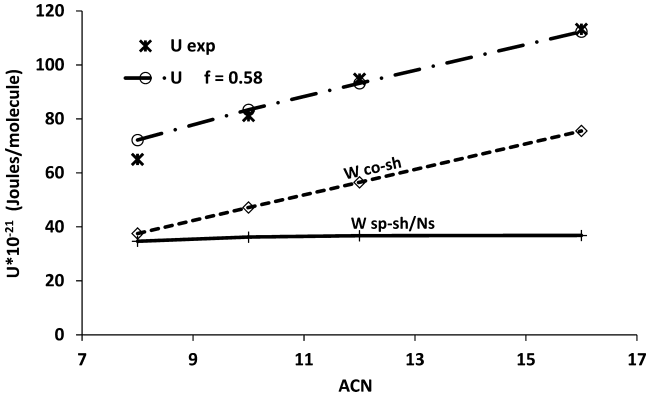

Figure 11. Predicted alkane cohesive energies (dot + dash line) calculated using the Lifshitz-based Hamaker constant. The dashed line (Wco-sh) represents the cone-shell contribution to the calculated cohesive energy. The solid line (Wsp-sh) represents the sphere-shell contribution. Experimental cohesive energies (Uexp. internal energy of vaporization) were calculated from experimental values of enthalpies of vaporization at 25 °C.

and smaller hydrocarbons are not included in these predictions due to the fact that they produce inner spheres of 1 nm in size or smaller, for which the sphere approximation of the micelle shell does not apply. As expected, the cohesive energy increases

dx.doi.org/10.1021/jp305534d | J. Phys. Chem. B 2012, 116, 14051−14061

with increasing ACN, mainly because the cone-shell interaction potential increases with ACN. The sphere-shell interaction potential provides a complementary amount of the cohesive energy.

For the sphere-shell interaction potential, a single interfacial separation distance was used as suggested by Israelachvili.[1] However, for the cone-shell configuration, it is impossible to assign a single separation distance due to the divergent separation distances arising from this geometry. Instead, we defined in section 2.2 a distance that is dependent on the angle of the cone and the packing conditions through a factor f that has been determined to be 0.58 for the n-alkanes considered in this study. Thus, the longer the hydrocarbon chain length, the smaller the separation angle between the cone and the coneless shell. However, the average interfacial separation distances, between the cone and the shell, remain about the same as a result of a balance of separation angles and chain lengths. The interfacial separation distances, for the components studied here, are reported as the average between the longest and the shortest distances that separate the cone and the shell. These distances are reported in Table 5 and are of the same magnitude to the 0.165 nm reported in the literature.[1,12]

Table 5. Average Interfacial Separation Distances between the Cone and the Shell for Different Alkanes

component	δ_{AV} (nm)
C8	0.156
C10	0.157
C12	0.158
C16	0.159

4. CONCLUSIONS

Two interbody unretarded VDW interaction potentials have been introduced, one for a sphere with a shell and a second one for a cone with a shell. Both potentials are presented as explicit expressions that can be solved using numerical methods. The sphere-shell interaction potential has no fitting parameters, while the cone-shell's separation distance has been established to be dependent on a cone-angle separation factor, f. This separation factor, assessed from experimental values of cohesive energies, leads to an average interfacial separation distance between the cone and the shell of 0.158 nm that compares well with the 0.165 nm proposed in the literature. It was confirmed that retardation effects were not important for these short interfacial separations, but they are significant at separations larger than 10 nm.

The sphere-shell interaction potential calculated using the classical Hamaker constant predicts the surface tension of the alkanes studied here at 20 °C with an average error of about 12%. The surface tensions calculated using the Lifshitz-based Hamaker constant produce an average prediction error of less than 3% for the same alkanes. Combining the sphere-shell and cone cone-shell interaction potentials proposed in this work calculated using the Lifshitz-based Hamaker constant and the adjusted separation factor produced cohesive energies that are within less than 4% of the experimental values at 25 °C.

APPENDIX: RETARDATION EFFECTS IN SPHERE-SHELL INTERACTIONS

The VDW retarded interaction between two bodies can be calculated using the Casimir and Polder potential.[30] Because of the complexity of this potential, it is customary to use a simple correction factor to the interaction parameter constant expressed as follows:[9,31]

$$w_R(r) = \frac{-C}{r^n} f(P) \tag{A1}$$

where $w_R(r)$ represents the VDW retarded interaction potential between two molecules and $f(P)$ is the correction factor as proposed by Overbeek, which for $0 < P < 3$ is[31]

$$f(P) = 1.10 - 0.41P \tag{A2}$$

P is a function of a reduced distance as given by:[30]

$$P = \frac{2\pi r}{\lambda} \tag{A3}$$

where λ is the characteristic wavelength of the interaction, which is usually assumed to be 100 nm.[31] The VDW retarded interaction potential of a sphere with a molecule is calculated using the procedure presented in section 2.1, which can be written as:

$$\varphi_{H-R}(D_o) = \frac{-\rho_1 C\ 4.4\pi {R_o}^3}{3[(D_o + R_o)^2 - {R_o}^2]^3} + \frac{-\rho_1 C\ 1.12\pi^2 {R_o}^3}{3\lambda {D_o}^2 (D_o + R_o)(D + 2R_o)^2} \tag{A4}$$

Using eq A4 and multiplying the volume of the shell in a manner previously described in section 2.1, the retarded interaction potential of a sphere with a shell is given by the following expression:

$$W_{H-R}(D) = \frac{-\rho_1\rho_2\ 17.6\pi^2 {R_o}^3 C}{3} \int_{R_o+D}^{R_o+D+L} \frac{\zeta^2 d\zeta}{(\zeta^2 - {R_o}^2)^3} + \frac{\rho_1\rho_2\ 4.48\pi^3 {R_o}^3 C}{3\lambda} \int_{R_o+D}^{R_o+D+L} \frac{\zeta^2\, d\zeta}{\zeta(\zeta^2 - {R_o}^2)^2} \tag{A5}$$

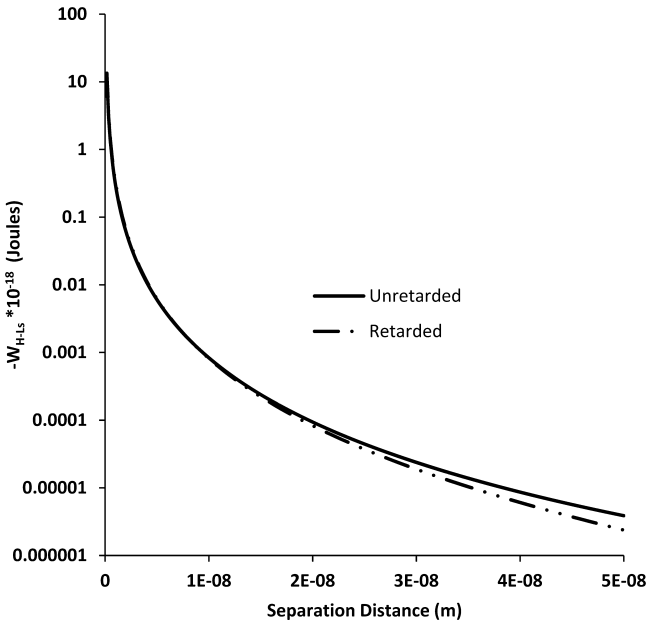

Figure A1. Retarded and unretarded sphere-shell interaction potentials estimated using the Lifshitz-based Hamaker constant for hexadecane at 20 °C with a sphere radius of 5 nm and shell's layer length of 2.17 nm.

dx.doi.org/10.1021/jp305534d | J. Phys. Chem. B 2012, 116, 14051−14061

When comparing the retarded and unretarded sphere-shell interaction potentials using the Lifshitz-based Hamaker constant for Hexadecane, retardation effects appear at separation distances beyond 10 nm as shown in Figure A1.

Calculations, equivalent to the ones presented in Figure A1 for hexadecane, were also obtained for octane and dodecane in sphere-shell configurations. Similarly, for separations below 10 nm, there was no appreciable difference between the retarded and the unretarded interactions.

AUTHOR INFORMATION

Corresponding Author

*Tel: 416-946-0742. Fax: 416-978-8605 . E-mail: acosta@chem-eng.utoronto.ca.

Notes

The authors declare no competing financial interest.

NOMECLATURE

List of Acronyms and Symbols

A: Hamaker constant
A_{ls}: Hamaker constant based on the Lifshitz's theory
A_o: surface area of the of the wider base of the cone
ACN: alkane carbon number
C: interaction coefficient
D: interbody separation distance
d_o: radius of an empty hollow of a sphere or excluded volume of a hypothetical micelle
D_o: distance between a hard sphere molecule and a sphere
f: a constant that defines the separation distance between a cone and a shell
h: Planck's constant
I_A: first ionization potential of molecule A
I_B: first ionization potential of molecule B
L: straight chain length of alkanes
n: integer expressing the exponential decay of an interaction with distance
n_i: refractive index
N: Avogadro's number
N_s: the aggregation number of a shell
r: distance between two molecules or two bodies
r_s: external radius of a truncated cone
R': a variable obtained using the chord theorem
R_o: radius of the sphere
T: temperature
U: cohesive energy
VDW: van der Waals
VLE: vapor liquid equilibrium
V_i: volume of interacting bodies
V_o: molecular volume of a molecule
$V(r)$: generic expression to define the interaction of two bodies
$w(r)$: pair interaction potential between molecules
$W(R_o)$: interaction between a liquid sphere and a liquid shell as a function of the sphere size
$W_H(R_o)$: sphere-shell interaction in the liquid phase calculated using the classical Hamaker constant
$W_{H-Ls}(R_o)$: sphere-shell interaction in the liquid phase calculated using the Lifshitz-based Hamaker constant
$W_{H-R}(D)$: retarded sphere-shell interaction calculated using the classical Hamaker constant
x: variable used to define the volume element of a ring and the volume element of a truncated cone
y: variable used to define the volume element of a coneless shell
z: variable used to define the volume element of a ring and the volume element of a truncated cone

Greek Letters

α: variable in spherical coordinates used to define the volume element of a coneless shell
α_p: molecular polarizability
α_{PA}: molecular polarizability of molecule A
α_{PB}: molecular polarizability of molecule B
α_1: angle that defines the radius of a cone
α_2: initial limit of integration of the coneless shell
δ: interfacial separation distance define to be 0.165 nm
δ_{av}: average separation distance between the cone and the coneless shell
δ_T: temperature-dependent interfacial separation distance
ΔH^V: enthalpy of vaporization
ΔU^V: difference between the internal energies of the vapor and liquid
ε: dielectric constant
ε_l: dielectric constant of liquids as a function of temperature
ε_o: vacuum permittivity
γ: surface tension
γ_e: characteristic absorption frequency
γ_{exp}: experimental surface tension
γ_H: surface tension calculated using the sphere-shell interaction based on classical the Hamaker constant
γ_{H-Ls}: surface tension calculated using the sphere-shell interaction based on the Lifshitz-based Hamaker constant
Γ: interaction between a truncated cone and a shell
Γ_{H-Ls}: interaction between a truncated cone and a shell using the Lifshitz-based Hamaker constant
κ: Boltzmann constant
ϕ: variable in spherical coordinates used to define the angle of a cone
$\varphi(R_o)$: interaction between a hard sphere molecule and a sphere as a function of the sphere size
$\varphi_{H-R}(D_o)$: retarded interaction between a hard sphere molecule and a sphere as a function of distance
$\Omega(R_o)$: interaction between a liquid sphere and a gas shell
ρ_i: molecular density per unit volume
ρ_m: molar density of the gas
σ: diameter of a hard sphere molecule
ξ: variable used to define a volume element of a spherical shell

REFERENCES

(1) Israelachvili, J. N. *Intermolecular and Surface Forces*, 3rd ed.; Elsevier: New York, 2011.

(2) Butt, H.-J.; Kappl, M. *Surface and Interfacial Forces*; Wiley-VCH Verlag Gmbh & Co. KGaA: Weinheim, Germany, 2010.

(3) Parsegian, V. A. *Van der Waals Forces: A Handbook for Chemists, Engineers, and Physicists*; Cambridge University Press: Cambridge, 2006.

(4) Ninham, B. W.; Lo Nostro, P. *Molecular Forces and Self Assembly in Colloid, Nano Sciences and Biology*; Cambridge University Press: Cambridge, 2010.

(5) Yildirim Erbil, H. *Surface Chemistry of Solid and Liquid Interfaces*; Blackwell Publishing: Oxford; Malden, MA, 2006.

(6) Tadmor, E. The London-Van der Waals Interaction Energy between objects of Various Geometries. *J. Phys.: Condens. Matter* **2001**, *13*, L195–L202.

(7) Eun-Suok, O. Van der Waals Interaction between Non Planar Bodies. *Korean J. Chem. Eng.* **2004**, *21* (2), 494–503.

(8) Tcholakova, S.; Denkov, N. D.; Borwankar, R.; Campbell, B. Van der Waals Interaction between Two Truncated Spheres Covered by a Uniform Layer (Deformed Drops, Vesicles, or Bubbles). *Langmuir* **2001**, *17*, 2357−2362.
(9) Gu, Y.; Li, D. The Van der Waals Interaction Between a Spherical Particle and a Cylinder. *J. Colloid Interface Sci.* **1999**, *217*, 60−69.
(10) Kirsch, V. A. Calculation of the van der Waals Force between a Spherical Particle and an Infinite Cylinder. *Adv. Colloid Interface Sci.* **2003**, *104*, 311−324.
(11) Hamaker, H. C. The London-Van der Waals Attraction Between Spherical Particles. *Physica* **1937**, *4* (10), 1058−1072.
(12) Su, Z.-Y.; Flumerfelt, R. W. A Continuum Approach to Microscopic Surface Tension for the n-Alkanes. *Ind. Eng. Chem. Res.* **1996**, *35*, 3399−3402.
(13) Winsor, P. A. Binary and Multicomponent Solutions of Amphiphilic Compounds. Solubilization and the Formation, Structure, and Theoretical Significance of Liquid Crystalline Solutions. *Chem. Rev.* **1968**, *68* (1), 1−40.
(14) Lide, D. R., Ed. *CRC Handbook of Chemistry and Physics*, 75th ed; CRC Press: New York, 1995.
(15) Sent, A. D.; Anicich, V. G.; Arakelian, T. Dielectric Constant of liquid Alkanes and Hydrocarbon Mixtures. *J. Phys. D: Appl. Phys.* **1992**, *25*, 516−521.
(16) Kirsh, V. A. The effect of van der Waals' Forces on Aerosol Filtration with Fibrous Filters. *Colloid J.* **2000**, *62* (6), 714−720.
(17) Rosen, M. J. *Surfactants and Interfacial Phenomena*, 3rd ed.; John Wiley & Sons: New York, 2004.
(18) Israelachvili, J. N.; Mitchell, D. J.; Ninham, B. W. Theory of self-assembly of hydrocarbon amphiphiles into micelles and bilayers. *J. Chem. Soc., Faraday Trans. 2* **1976**, *72*, 1525−1568.
(19) Tanford, C. *The Hydrophobic Effect*; John Wiley & Sons: New York: 1980.
(20) Lemmon, E. W.; McLinden, M. O.; Friend, D. G. Thermophysical Properties of Fluid Systems. In *NIST Chemistry WebBook, NIST Standard Reference Database Number 69*; Linstrom, P. J., and Mallard, W. G., Eds.; National Institute of Standards and Technology: Gaithersburg, MD; 20899, http://webbook.nist.gov (retrieved May 29, 2012).
(21) Melton, C. J.; Joy, H. W. Ionization Potentials of alkyl free Radicals and *n*-Alkanes through $C_{17}H_{36}$ by Energy-Calibrated Molecular orbital methods. *Can. J. Chem.* **1966**, *44*, 1455−1462.
(22) Miller, K. J.; Savchik, J. A. A New Empirical Method to Calculate Average Molecular Polarizabilities. *J. Am. Chem. Soc.* **1979**, *101* (24), 7206−7213.
(23) Outcalt, S.; Laesecke, A.; Fortin, T. J. Density and Speed of Sound measurements of hexadecane. *J. Chem. Thermodyn.* **2010**, *42*, 700−706.
(24) Philip, J. D.; Rabinowitz, P. *Methods of Numerical Integration*, 2nd ed.; Academic Press: Orlando, 1984.
(25) Tolman, R. C. The effect of Drop Size on surface tension. *J. Chem. Phys.* **1949**, *17*, 333−337.
(26) Grigoryev, B. A.; Nemzer, B. V.; Kurumov, D. S.; Sengers, J. V. Surface Tension of Normal Pentane, Hexane, Heptane and Octane. *Int. J. Thermophys.* **1992**, *13* (3), 453−464.
(27) Jasper, J. J.; Kring, E. V. The Isobaric Surface Tensions and Thermodynamic Properties of the Surfaces of a Series of *n*-Alkanes, C_5 to C_{18}, 1-Alkenes, C_6 to C_{16}, and of *n*-Decylcyclopentane, *n*-Decylcyclohexane and *n*-Dcylbenzene. *J. Phys. Chem.* **1955**, *59* (10), 1019−1021.
(28) Maffiolo, G.; Vidal, J.; Renon, H. Cohesive Energy of Liquid hydrocarbons. *Ind. Eng. Chem. Fundamen.* **1972**, *11* (1), 100−105.
(29) Jovanovic, J. D.; Grozdanic, D. K. Reliable Prediction of heat of Vaporization of *n*-alkanes at 298.15 K. *J. Serb. Chem. Soc.* **2010**, *75* (7), 997−1003.
(30) Casimir, H. B. G.; Polder, D. The Influence of Retardation on the London-van der Waals Forces. *Phys. Rev.* **1948**, *73* (4), 360.
(31) Gregory, J. Approximate Expressions for Retarded van der Waals Interaction. *J. Colloid Interface Sci.* **1981**, *83* (1), 138−145.